Gasohol Sprays Simulations of a Multi-Hole GDI Injector in Engine-Like Conditions

Conference Paper *in* SAE Technical Papers · April 2021

DOI: 10.4271/2021-01-0549

3 authors:

Ankur Kalwar
Indian Institute of Technology Kanpur

Sam Chintagunti
Indian Institute of Technology Kanpur

Avinash Kumar Agarwal
Indian Institute of Technology Kanpur

2021-01-0549 Published 06 Apr 2021

Gasohol Sprays Simulations of a Multi-Hole GDI Injector in Engine-Like Conditions

Ankur Kalwar, Sam Chintagunti, and Avinash Kumar Agarwal Indian Institute of Technology - Kanpur

Citation: Kalwar, A., Chintagunti, S., and Agarwal, A.K., "Gasohol Sprays Simulations of a Multi-Hole GDI Injector in Engine-Like Conditions," SAE Technical Paper 2021-01-0549, 2021, doi:10.4271/2021-01-0549.

Abstract

Mixture formation in GDI engine is considered crucial in determining combustion and emissions characteristics, which mainly depend on fuel spray quality. However, spray characteristics change with variations in control parameters such as fuel injection parameters, fuel injection strategy, engine operating conditions, and fuel properties. Growing research interest in the use of methanol as an additive with gasoline has motivated the need for deeper investigations of spray characteristics of these fuels. Although, it can be noted that sufficient literature is available in the area of spray characterization under several independent influencing factors, however, comparative analysis of gasohol spray behavior under different ambient conditions is hardly studied. This study is aimed at investigating the spray morphology, and evaporation and mixing characteristics of M15 (15% v/v methanol in iso-octane) and M85 (85% v/v methanol in iso-octane) in comparison to iso-octane at early injection and late injection conditions. CFD simulation studies were performed using multi-hole GDI injector in a constant volume spray chamber (CVSC) using Converge software. Numerical model used for the analysis was validated using experimental spray penetration measurements, available at the ECN. The results highlighted that effect of methanol properties on spray penetration and SMD of fuel droplets diminished under high temperature-high pressure conditions. Although, substantial difference in droplets evaporation was found among the test fuels due to inferior volatility of methanol, which definitely demands optimization of fuel injection parameters for adapting methanol blends in the engine. However, despite lower droplet evaporation, equivalence ratio distribution for methanol blends was more shifted towards stoichiometric conditions due to inherent fuel oxygen content.

Keywords

Gasoline Direct Injection, Simulation, Spray Characteristics, Methanol, Mixture Formation

Introduction

One of the major crisis the world is facing right now is climate change. It can be combated to a great extent by reducing the vehicular pollution and making internal combustion (IC) engines more efficient. Majority of passenger car fleet in the automotive sector is dominated by spark-ignition engines. Hence research emphasis and technological developments in gasoline fueled vehicles are aimed at developing efficient and cleaner combustion technologies [1]. Gasoline direct injection (GDI) technology utilizes the advantages of both, diesel and gasoline engines to achieve efficient and high-performance engine combustion. In GDI engines, fuel is injected directly into the engine combustion chamber either during the intake stroke, or towards the end of the compression stroke depending on the load and mode of engine operation. This enables precise control and large window for fuel injection timing, which leads to different fuel-air mixture compositions depending on the engine operating requirements. However, the reduced time for fuel-air mixing makes this phenomenon complex [2,3]. It was estimated that global volume GDI engine equipped vehicles will surpass the global volume of PFI engine equipped vehicles by 2020 because of its better performance especially at part load conditions in addition to reduced throttling losses compared to the PFI engines [3]. GDI engines are known for higher power density, better fuel economy and lower CO_2 emissions because of their ability to achieve ultra-lean combustion and this is possible because of a good control over mixture formation [4]. These advantages and complexities make the study of mixture formation very important for improving its limitations, which include combustion instability, and higher particulate and NOx emissions.

Fuel-air mixture formation depends on various factors such as fuel injection parameters, ambient conditions, fuel properties, air motion, injector design. Many studies have been done to understand the impact of these factors on spray characteristics and subsequent fuel-air mixing process [5, 6, 7]. Lee et al. [8] reported branch like structures, which formed due to air entrapment in the fuel sprays. These structures formed more rapidly at higher fuel injection pressure (FIP), facilitating further disintegration of spray droplets, thus improving the spray atomization process. In addition, higher FIP shifted the droplet diameter distribution towards smaller droplets. However, no significant reduction in droplet diameter was found beyond 20 MPa FIP. Spray penetration is an important parameter to characterize the fuel-air mixing phenomenon. It was reported that spray penetration increases with increasing FIP [9], however in another study [10], author reported no increase in the spray penetration beyond certain FIP was reported due to increased spray-air momentum transfer. Improved fuel spray droplet atomization resulted in lower PM, PN and HC emissions, superior fuel economy and reduced cyclic variations. Similarly, ambient pressure and temperature conditions also play an important role on the spray morphology and mixture formation. Tian et al. [11] reported that under high ambient pressure conditions, spray head was wider and axially compressed for vaporizing sprays due to greater flow resistance. In these vaporizing conditions, vapor penetration behaved similar to liquid penetration however it was a little behind it. It later surpassed due to vaporization. As FIP increased, the point where two-phase penetration coincided came closer to the nozzle, which again suggested superior fuel droplet evaporation and air entrainment with increasing FIP. Compared to diesel spray, gasoline spray penetration was largely dependent on ambient air density in comparison to injection pressure differential. Similar observation was reported by Mitroglou et al. [9] that increase in ambient pressure from ambient to 12 bar had much significant effect on reduction in fuel droplet size, when compared to increase in FIP upto 200 bar. Furthermore, many research studies suggested that ambient pressure and temperature states are critically responsible for spray collapse phenomenon in the multi-hole GDI sprays [12,13]. In one such study [14], authors reported near-field spray collapse at elevated ambient pressure conditions and far-field spray collapse at flash boiling conditions. They inferred that increased jet-air interactions at high ambient pressure resulted in low pressure zone near the injector tip and induced spray collapse. While in the flash boiling conditions, condensation of fuel vapors due to temperature drop during surface evaporation caused low pressure zone in far-field, resulting in spray collapse. Flash boiling enhanced at higher fuel temperatures. Significant research is underway to utilize the phenomenon of condensation-induced spray collapse for better fuel-air mixture formation, especially in homogeneous mode of GDI engines.

With strict targets of emissions norms, researchers are also investigating the performance of biofuels in improving the combustion characteristics, while limiting the emissions from engines. Alcohols are emerging as an important category of biofuels, which can be generated from coal, natural gas, and also from biomass waste gasification [15]. Among alcohols, methanol has least carbon content and maximum oxygen content, which has significant effect in reducing the particulates and other carbon-based emissions from GDI engines [16]. Methanol is being used in automobiles in many countries, especially in USA and China. It is the cheapest alternative liquid fuel per unit energy content and has excellent combustion properties, which make it relevant for application in spark ignition (SI) engines [17]. Although positive and negative impact of its properties depends on the blending percentage in gasoline as well as operating parameters of the engine. Hence, several studies have been attempted in the past to characterize the effect of different alcohols on the spray characteristics and mixing properties, in order to increase their adaptability in IC engines [18,19]. In one such study [20], authors reported that effect of fuel properties on spray penetration was dependent on fuel injection conditions. They investigated the effect of varying FIP (4-15 MPa) onto spray evolution of ethanol, gasoline, and iso-octane. At lower FIP, increased nozzle losses due to higher density and viscosity of ethanol resulted in lower injection velocity, hence lower spray penetration. However, penetration of ethanol spray surpassed that of gasoline at high FIP due to larger droplet sizes and reduced aerodynamic drag. Kale et al. [21] analyzed the effect of thermo-physical properties of ethanol and n-butanol on spray morphology w.r.t. iso-octane at elevated pressure and temperature conditions.

Because of availability of extensive experimental datasets, accurate CFD modeling of various complex phenomenon of fuel sprays has been possible to a great extent [22]. Several studies were conducted for calibration and tuning of CFD models for validating different spray characteristics [23,24]. Although, experimental studies are more reliable in terms of accuracy, they have their own limitations in detailed analysis. Despite of availability of series of publications in open domain, scientific studies attempted so far have not accounted for gasohol sprays at engine-like conditions resembling GDI engine operation at varying loads. In addition, the effect of high premixing ratio of methanol on the gasoline spray is not investigated. Hence this study aims at characterizing spray modelling for methanol-iso-octane blends w.r.t. iso-octane under two ambient conditions resembling homogeneous (early injection) and stratified (late injection) modes of GDI engine.

Computational Setup

The test conditions for this study were taken in accordance with ECN standard conditions for gasoline sprays. ECN has set standard operating conditions for the analysis of multi-hole GDI sprays so that it remains consistent for all studies performed by different research groups and advantage of large database created can be taken. The simulations were performed at two different engine-like conditions common to GDI engine operation, which are homogeneous mode at wide open throttle (early injection) and stratified mode (late injection). Ambient pressure and temperature conditions for these cases were as per ECN recommended values and are shown in Table 1, along with other operating parameters [25]. Injector specifications were considered for 8-hole GDI injector (Delphi) from ECN standard spray G case, as shown in Figure 1. The nozzle diameter of 170 μm, plume cone angle of 20° and plume direction along 37° relative to injector axis were considered for all simulations. Injection rate shape used in simulations from ECN

TABLE 1 Operating conditions for simulations

	Case A: Stratified Mode	Case B: Homogeneous Mode
Ambient temperature	573 K	333 K
Ambient pressure	6 bar (N_2)	1 bar (N_2)
Test fuels	Iso-octane, M15, M85	
Fuel injection pressure	200 bar	
Fuel injection quantity	10 mg	
Fuel injection duration	780 µs	
Fuel temperature	393 K	

FIGURE 1 Dimensions of ECN injector with 3D rendered drawing in upper right corner [25]

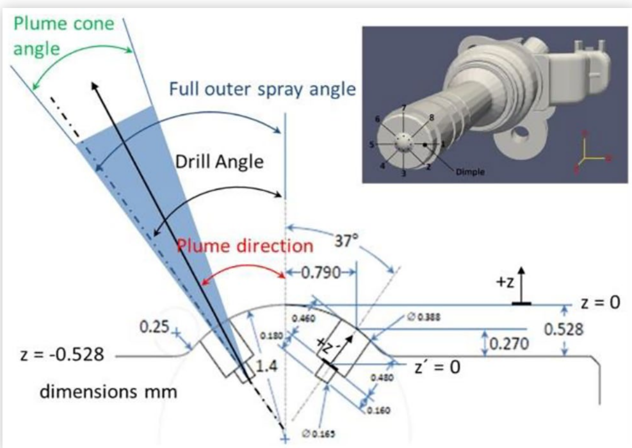

FIGURE 2 Fuel injection rate shape profile of ECN recommended injector [25]

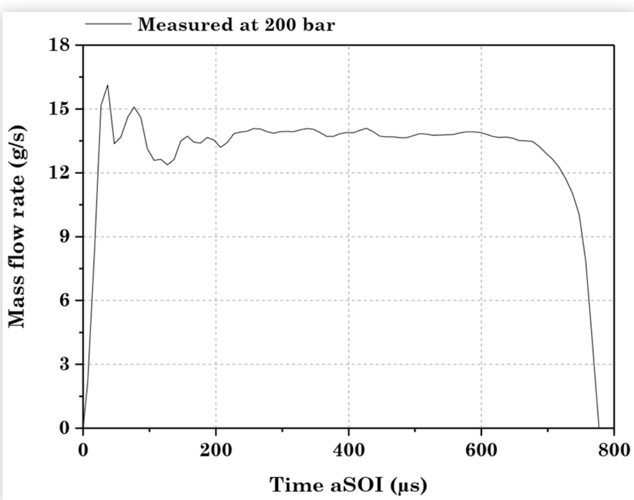

spray G database. To observe the behavior of methanol-gasoline blends in spray characteristics at different ambient conditions, three test fuels were considered for the study. M15 (15% v/v methanol in iso-octane) and M85 (85% v/v methanol in iso-octane) were chosen as test blends representing low and high premix-ratios of methanol, which were compared with baseline iso-octane (surrogate for gasoline). As per ECN standard spray G conditions, fuel temperature was taken to be 363 K and fuel injection quantity was maintained constant at 10 mg with injection duration of 780 µs for all test cases. The spray vessel comprised of only nitrogen, considering it as non-reacting spray.

Numerical Setup and Model Validation

Prediction of complete spray evolution for fuel-air mixture formation requires different sets of accurate sub-models for spray related phenomenon. Spray simulations were carried out using Converge 3.0 CFD software. Spray was modeled based on Lagrangian-Eulerian approach, where generated parcels of spray droplets were solved in Lagrangian mode and gaseous flow was modeled in Eulerian mode. Reynolds Averaged Navier-Stokes (RANS) RNG k-ε turbulence model was used for solving the turbulent governing equations. Spray droplets of size resembling nozzle diameter were simulated via blob-injection model, following which O'Rourke dispersion and kh-rt model were used to capture turbulent dispersion and breakup phenomenon of spray droplets. Evaporation of liquid fuel droplets was modeled using Frossling model and NTC collision model with a collision mesh of level 1 was used for simulating droplets collision phenomenon. The selection of these models was considered by referring to open literature related to ECN spray G validation [23,26]. Accuracy of these models was demonstrated by the results obtained in previous studies. Computational domain was discretized with base grid size of 4 mm. To resolve small scale of turbulence, Adaptive Mesh Refinement (AMR) on the basis of velocity gradient and fixed embedding near injector were employed with a scale factor of 4. The minimum cell size in the domain was 0.25 mm. Discharge coefficient of the nozzle and parcels per plume were taken to be 0.54 and 10000 respectively. The simulation time of 2 ms was considered, which was beyond the injection duration to analyze after-injection characteristics. Computational domain and details of adopted sub-model constants for numerical setup are shown in Figure 3 and Table 2. The adopted numerical setup

FIGURE 3 Computational domain for the Constant Volume Spray Chamber (CVSC).

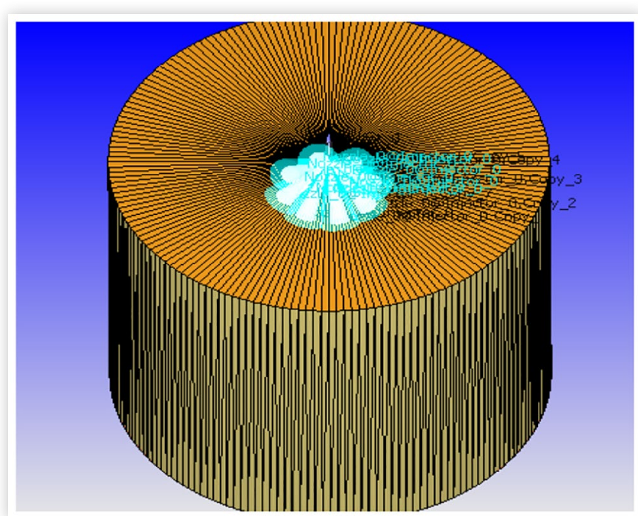

TABLE 2 Details of adopted sub-model constants for numerical setup

Plume cone angle	20°
Plume direction angle	37°
RANS constants	C_μ = 0.0845, $C_{\varepsilon1}$ = 1.42, $C_{\varepsilon2}$ = 1.68, $C_{\varepsilon3}$ = -1.0
KH constants	Model size constant (B_o) = 0.6 Model breakup time constant (B_1) = 7.0
RT constants	Model breakup time constant (C_τ) = 1.0 Model size constant (C_{RT}) = 0.6
Initial Turbulent Kinetic Energy	k = 1 m^2/s^2
Initial TKE dissipation rate in the region	ε = 100 m^2/s^3

was kept same for both, the Stratified mode and the Homogeneous mode. This was done in order to ensure the capability of the proposed model to predict spray and mixture formation characteristics in a complete GDI engine cycle, which comprised both of stratified and homogeneous operations. Similar approach was used in previous studies also [23].

For validation of the CFD case setup, liquid and vapor spray penetration of iso-octane at ECN standard spray G1 condition (T_{amb} = 573 K & P_{amb} = 6 bar) and G3 condition (T_{amb} = 333 K & P_{amb} = 1 bar) were validated with experimental data provided by the Sandia Group and the University of Melbourne (UOM) [25]. Low threshold profiles of experimentally obtained liquid penetration length were used for validating both, the iso-octane G1 and G3 cases. The liquid penetration was obtained numerically with 95% threshold for liquid fuel mass fraction and vapor penetration was computed on the basis of 0.1% of fuel vapor mass fraction. All other operating parameters were similar as mentioned previously. Figure 4a and 4b showed the simulated and experimental results of iso-octane liquid and vapor spray penetrations for stratified mode and homogenous mode respectively. The graphs clearly showed the validation of the adopted numerical model for both conditions. Figure 5 showed the isometric and cross-sectional views of spray parcels indicating droplet temperature at stratified condition, which represents the spray morphology.

FIGURE 4a Validation of liquid and vapor spray penetration (at T_{amb} = 573 K & P_{amb} = 6 bar) showing both experimental (Sandia group) and simulation results (Present study).

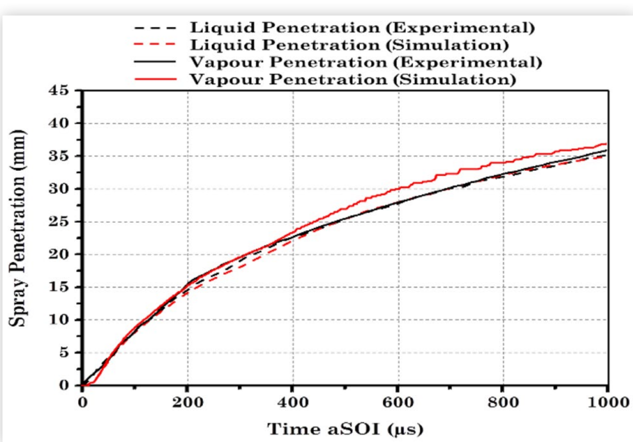

FIGURE 4b Validation of liquid and vapor spray penetration (at T_{amb} = 333 K & P_{amb} = 1 bar) showing both experimental (UOM group) and simulation results (Present study).

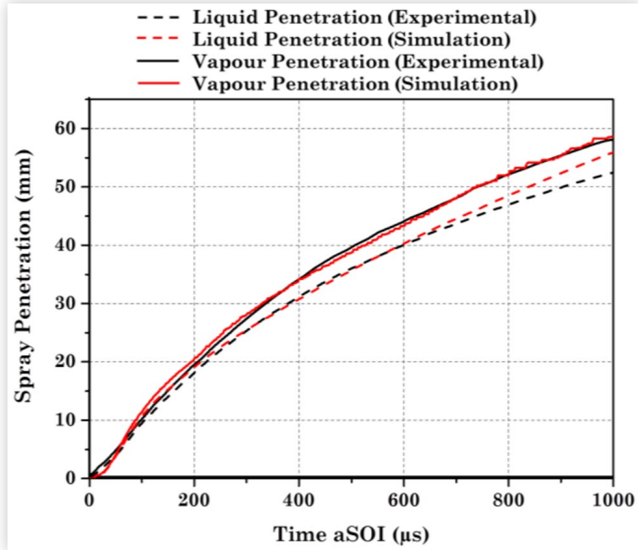

FIGURE 5 Isometric and cross-sectional views of Spray parcels indicating droplet temperature (at T_{amb} = 573 K & P_{amb} = 6 bar).

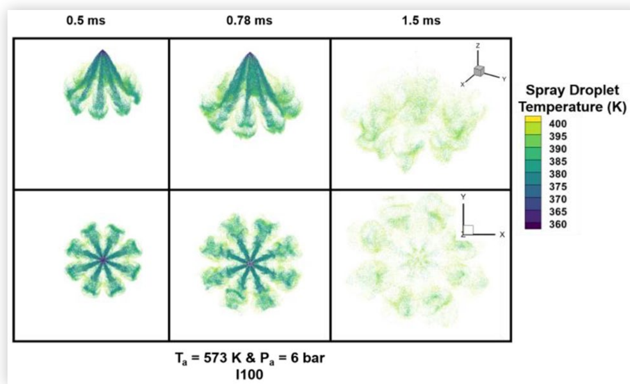

Results and Discussion

The spray behavior of methanol-iso-octane blends for early-injection (homogeneous mode) and late-injection (stratified mode) conditions were investigated in terms of spray evolution, evaporation and mixture formation characteristics. Spray penetration and Sauter Mean Diameter (SMD) were obtained by determining spray characteristics. Liquid spray mass, temperature distribution and vapor mass fraction distribution were obtained from the evaporation characteristics. Finally, equivalence ratio contours were determined to analyze the mixture formation characteristics.

Spray Penetration

Figure 6a and 6b showed liquid and vapor spray penetrations respectively for all test fuels at two ambient conditions. General trend of the spray penetration length for all cases shows changing slope during initial period of injection. During initial phase of injection process, rate of spray penetration was generally higher due to greater spray stability and marginal interaction with ambient flow. Spray was mainly governed by its own momentum and velocity in this regime. However, once secondary breakup of the spray started, rate of penetration decreased due to increased droplets interaction with ambient gases [27]. This change of slope occurred earlier in case of higher temperature and pressure conditions due to an earlier breakup. Further, spray penetration was substantially lower in high temperature/ pressure condition. Increased ambient pressure resulted in greater drag and resistance to spray penetration. In addition, high ambient temperature led to increased evaporation of liquid droplets. These spray characteristics are desirable for stratified combustion mode in GDI engines. On the other hand, due to larger spray penetration, spray impingement is mostly observed in early injection (homogeneous mode) condition. The effect of methanol addition was only marginal in the spray penetration and that too at later phase of injection. Spray penetration increased slightly for methanol-gasoline blends due to higher density, viscosity, and surface tension of methanol as compared to iso-octane. Higher viscosity of methanol degraded spray atomization quality. Heavier droplets experienced lower drag forces, hence penetrated to longer distance by virtue of their momentum.

FIGURE 6a Variation of liquid spray penetration for all test fuels at different conditions: Stratified mode (T_{amb} = 573 K & P_{amb} = 6 bar) and Homogeneous mode (T_{amb} = 333 K & P_{amb} = 1 bar)

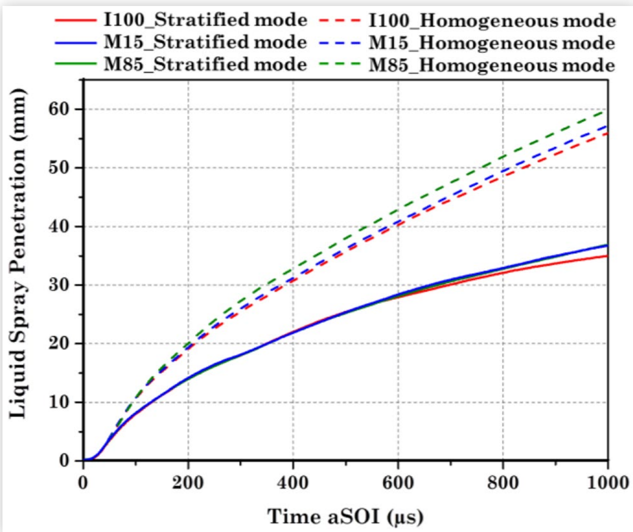

FIGURE 6b Variations of vapour spray penetration for all test fuels at different conditions: Stratified mode (T_{amb} = 573 K & P_{amb} = 6 bar) and Homogeneous mode (T_{amb} = 333 K & P_{amb} = 1 bar)

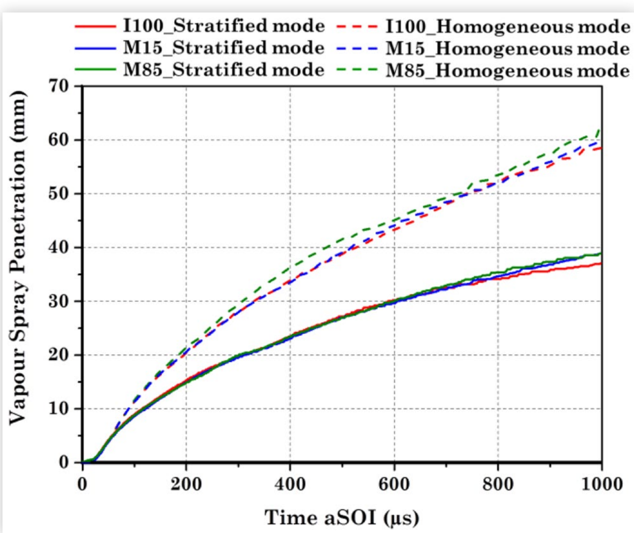

SMD Variations

Figure 7 shows variations of Sauter Mean Diameter (SMD) of spray droplets w.r.t. fuel injection duration. Numerical modeling of spray was based on blob concept, where spray droplets were introduced into the computational domain at the tip of nozzle. Droplets of size ~140 microns were reported at the start of injection after accounting for size reduction due to coefficient of contraction. With increasing time after the SOI, SMD of droplets decreased considering disintegration of larger droplets into smaller droplets. Sudden drop in SMD was observed for higher ambient temperature/ pressure conditions. It became almost stable in the range of 12-14 microns once primary breakup phase of spray was completed. Smaller droplet sizes were mainly a result of higher entrainment of

FIGURE 7 Variations of SMD for test fuels at different conditions: Stratified mode (T_{amb} = 573 K & P_{amb} = 6 bar) and Homogeneous mode (T_{amb} = 333 K & P_{amb} = 1 bar)

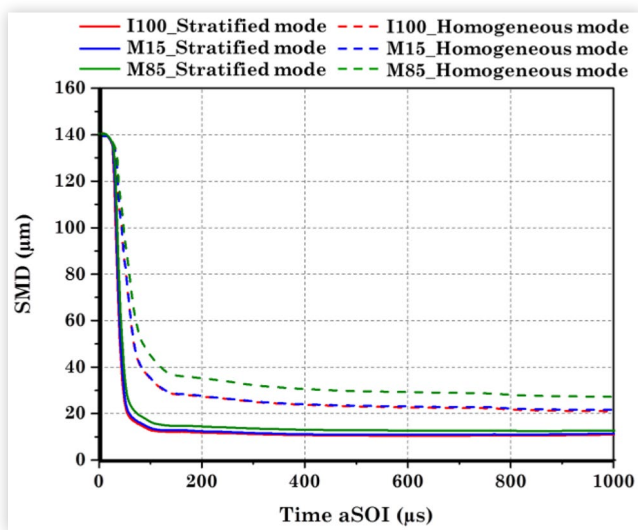

surrounding gases into the spray because of higher ambient density. Further, increased distortion of droplet shapes due to higher drag forces also resulted in enhanced spray breakup. In addition, high surrounding temperature might have also contributed to reduction of droplet size by enhancing surface evaporation of droplets. On the other side, for low ambient temperature and pressure condition, relatively slower and delayed primary breakup was observed. Continuous and small reduction in SMD was reported during the injection duration. Higher values of SMD in the range of 20-25 microns were certainly because of lower gas entrainment into the spray and reduced evaporation rate.

Considering the effect of methanol, lower blending fraction (M15) showed hardly any effect in high temperature/ pressure condition, while droplets marginally greater in size by few microns were reported in low temperature/ pressure condition. However, for higher blending fraction (M85), variations in SMD considerably enhanced for low temperature/ pressure condition. Droplets size increased for methanol blends due to their increased fuel viscosity and surface tension, compared to iso-octane. Owing to these fuel properties, spray breakup degraded slightly and resulted in bigger droplets. It can be inferred that effect of fuel properties diminished in elevated temperature/ pressure condition. Ambient conditions were dominant in controlling the spray breakup phenomenon.

Liquid Spray Mass Variation

Figure 8 highlights the evaporation characteristics of methanol-iso-octane blends at two different ambient conditions. Liquid spray mass kept on increasing till fuel injection, i.e. upto 780 µs, and then decreased depending on after-injection evaporation characteristics. It clearly depicts that high

FIGURE 8 Variations of liquid spray mass for test fuels at different conditions: Stratified mode (T_{amb} = 573 K & P_{amb} = 6 bar) and Homogeneous mode (T_{amb} = 333 K & P_{amb} = 1 bar)

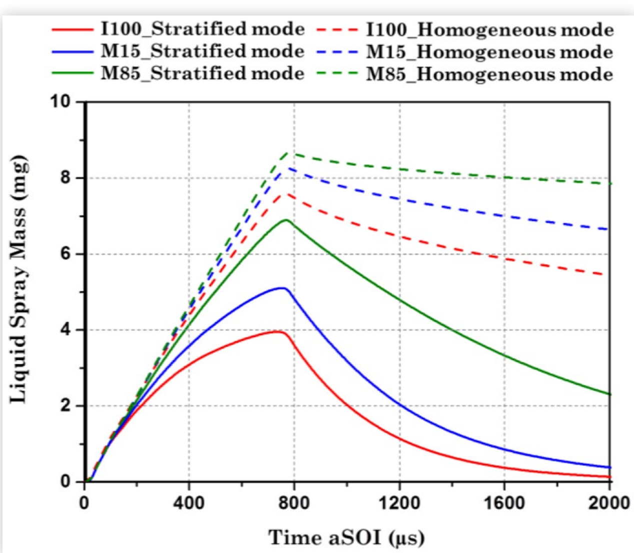

ambient temperature/ pressure conditions enhanced the evaporation of fuel droplets hence lower liquid spray mass was observed during the fuel injection. This could be because of superior spray atomization and entrainment of surrounding gases. Finer droplets provided larger surface area for heat transfer and greater temperature difference would have resulted in higher surface evaporation. After-injection evaporation was also more pronounced in this condition.

Iso-octane reported lowest liquid spray mass among test fuels in both conditions. Higher volatility of iso-octane due to its lower vapor pressure as compared to methanol was the main reason for its superior evaporation characteristics. In addition, higher fuel droplet size of methanol blends reduced the surface-to-volume ratio, which diminished the effective droplet surface area of energy exchange. Another major observation was that greater variation in liquid spray mass for the test fuels was reported in elevated ambient conditions. The slope of liquid spray mass kept on decreasing for iso-octane and M15 at this condition, which also indicated faster evaporation for these fuels. Hence, it can be inferred that fuel properties have considerable effect on the spray evaporation characteristics, which can significantly affect the fuel-air mixture quality. There was no substantial change in spray penetration for M15 and M85 compared to iso-octane. Spray droplets experienced almost similar momentum along the plume direction for a particular ambient condition, hence they were able to penetrate axially in a similar fashion. However, availability of whole lateral surface area of the spray for evaporation of droplets might have resulted in greater variation in liquid mass content.

Temperature Distribution

The cell temperature contours are shown in Figure 9 for late injection and early injection like ambient conditions. Effect of higher latent heat of vaporization of methanol was reflected in the cell temperatures at both conditions. In elevated ambient conditions, where ambient temperature and density were higher, effect of higher enthalpy of vaporization on cell temperature reduced for methanol blends. All test fuels showed similar ranges of temperature in all zones. This might be due to superior atomization and enhanced evaporation of gasoline over methanol under such conditions, which negated the effect of greater cooling due to vaporization of methanol. The cooler spots (dark blue spots) in M85 at 1.5 ms suggested that evaporation was still happening in M85 when other test fuels completed their evaporation. This might be due to larger droplets of methanol and lower volatility. In low ambient temperature/ pressure condition, low temperature region was spread over larger spray area, especially near the tip, indicating higher evaporation near the spray tip. Also, cooler regions first appeared in methanol blends, which indicated that though less fuel evaporated in the methanol blends, higher latent heat of vaporization of methanol dominated the cell temperature. To conclude, methanol blending with gasoline would produce cooler regions compared to gasoline, which increases volumetric efficiency of the engine.

FIGURE 9 Temperature distribution for test fuels at two ambient conditions: Stratified mode (T_{amb} = 573 K & P_{amb} = 6 bar) and Homogeneous mode (T_{amb} = 333 K & P_{amb} = 1 bar)

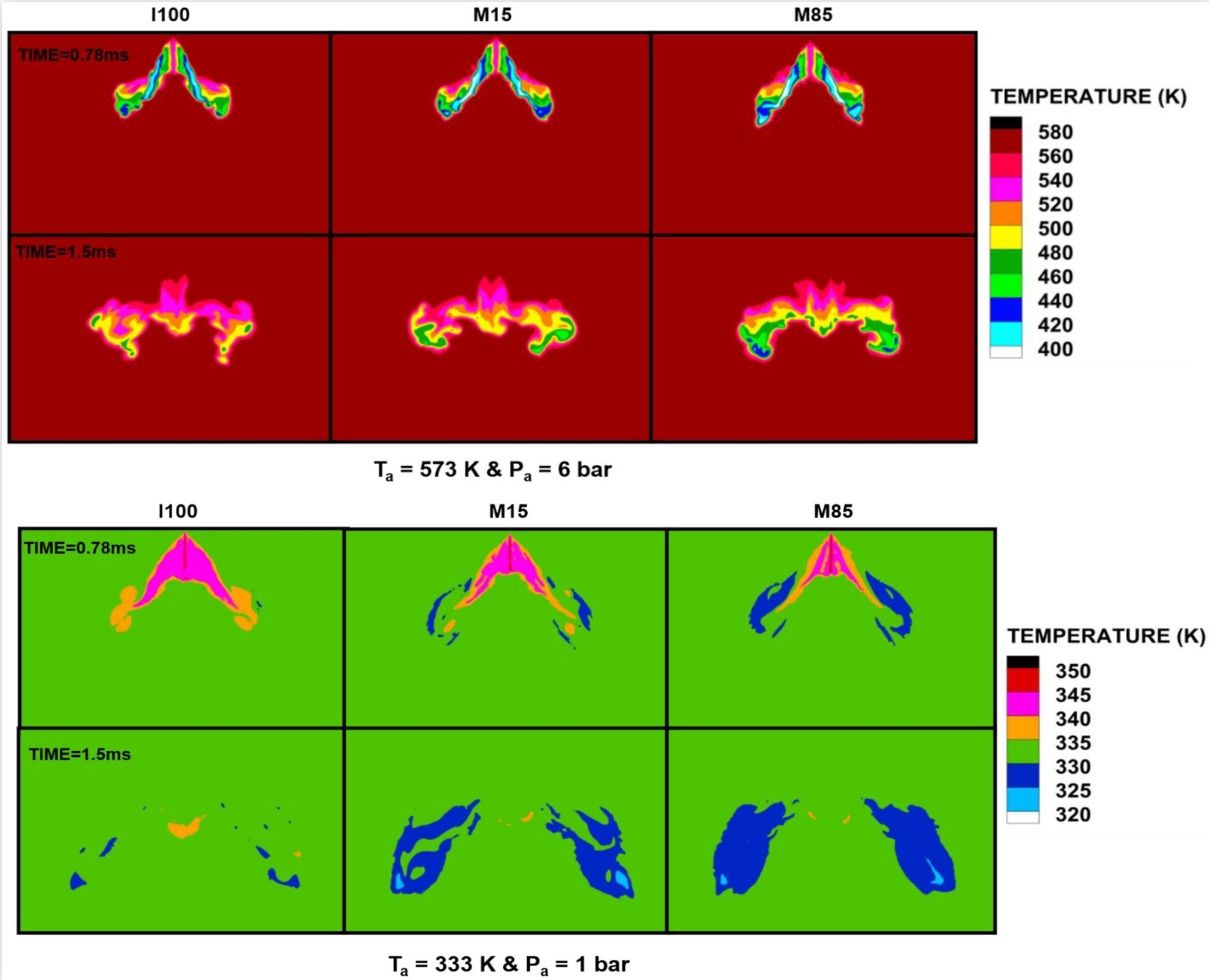

Vapor Mass Fraction Distribution

The contours of gaseous fuel mass fraction in Figure 10 gives an idea about how the evaporation is affected by fuel properties and ambient conditions. It is clear that iso-octane evaporates faster than methanol blends in both ambient conditions, represented by the higher gaseous fuel mass fraction. Increased ambient pressure/temperature increased the difference in evaporated fuel mass fraction. This supports the results obtained from liquid fuel mass curves (Figure 8). Hence, it can be inferred that the volatility and atomization of fuel droplets affects the evaporation of fuel spray and higher ambient density and temperature enhances this phenomenon. Higher ambient density enhanced the entrainment of hot surrounding gases into the spray. Hence, presence of higher ambient temperature and density augmented the fuel droplet evaporation characteristics.

Equivalence Ratio Distribution

The equivalence ratio contours in Figure 11 have showed a strong dependence on fuel properties. Equivalence ratio shown in these plots includes both, liquid and vapor fuel. Since Converge gives equivalence ratio based on vapor fuel only, relevant calculations were made in a similar fashion as previous work [26]. Oxygen content of methanol encourages mixture formation closer to stoichiometric. Though methanol blends exhibited larger spray droplets and slower evaporation compared to iso-octane, equivalence ratio remained closer to stoichiometric for methanol blends at both ambient conditions. This is an interesting observation,

FIGURE 10 Vapor mass fraction distribution for all test fuels at two ambient conditions: Stratified mode (T_{amb} = 573 K & P_{amb} = 6 bar) and Homogeneous mode (T_{amb} = 333 K & P_{amb} = 1 bar)

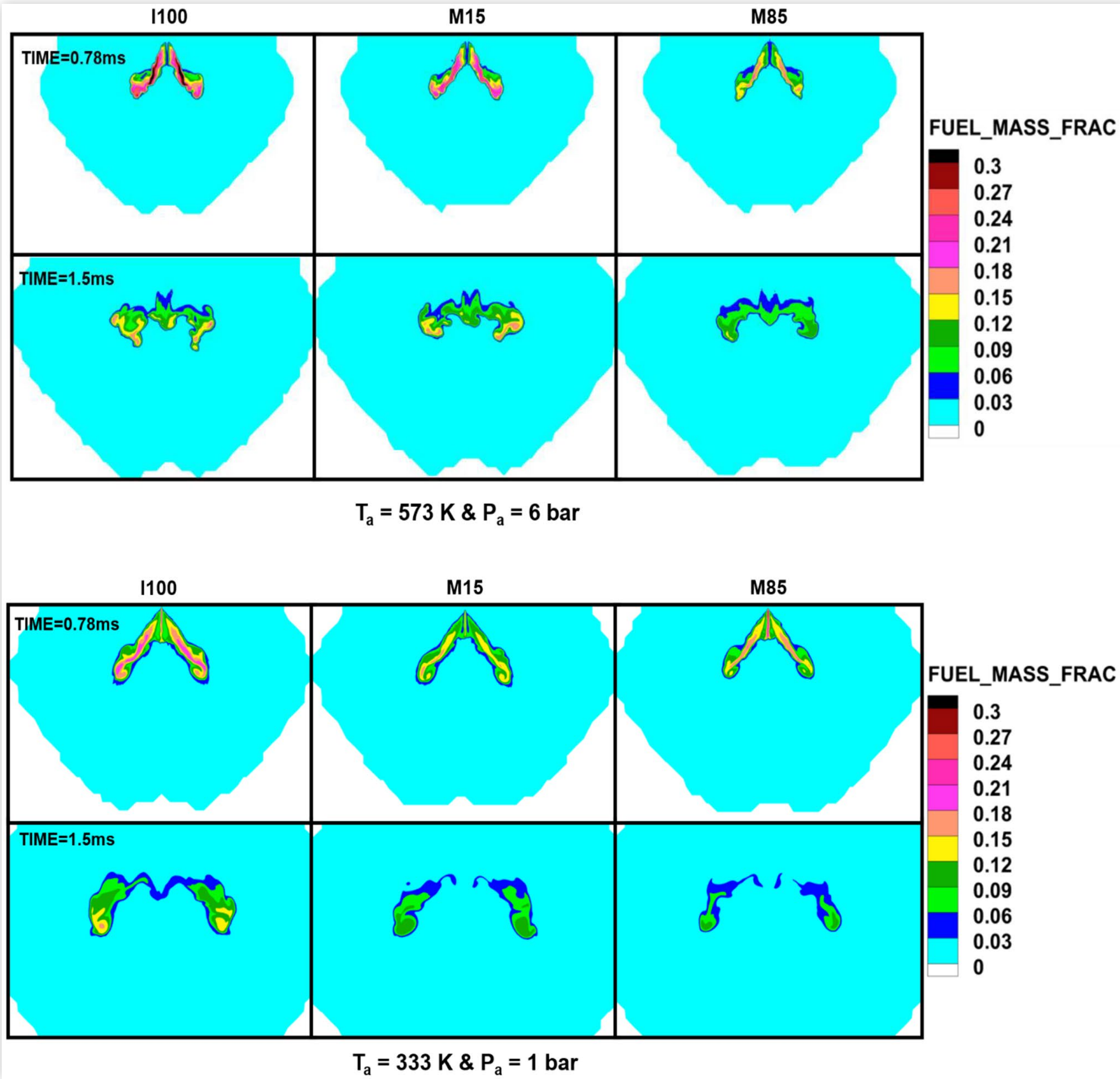

which plays an important role in the future of methanol as an alternative to IC engine fuels. Furthermore, under elevated ambient conditions, it was observed that the spray plumes were pushed towards the injector axis. This was because of the pressure difference created on both sides of the plume, especially in the high ambient pressure conditions. This was previously observed and highlighted in other studies as well [28,29]. Also, due to lower spray penetration under elevated conditions and the momentum of continuously injected fuel spray, liquid fuel seemed to reach till the end of the plume, which was indicated by the high equivalence ratio regions. It was observed that the stoichiometric region in late-injection condition seemed to reach into farther regions of the chamber compared to early-injection conditions at a given time. This might be due to higher resistance to the fuel spray in axial direction, causing more air entrainment, leading to superior fuel-air mixing and superior atomization and evaporation in late-injection conditions, that allowed superior diffusion of fuel in the combustion chamber. It is interesting to note that once the injection ended, region near the nozzle reached stoichiometric conditions more quickly compared to that at the spray tip. Spray head had richer fuel-air mixture and might be a potential source of particulate emissions.

FIGURE 11 Equivalence ratio distribution for all test fuels at two ambient conditions: Stratified mode (T_{amb} = 573 K & P_{amb} = 6 bar) and Homogeneous mode (T_{amb} = 333 K & P_{amb} = 1 bar)

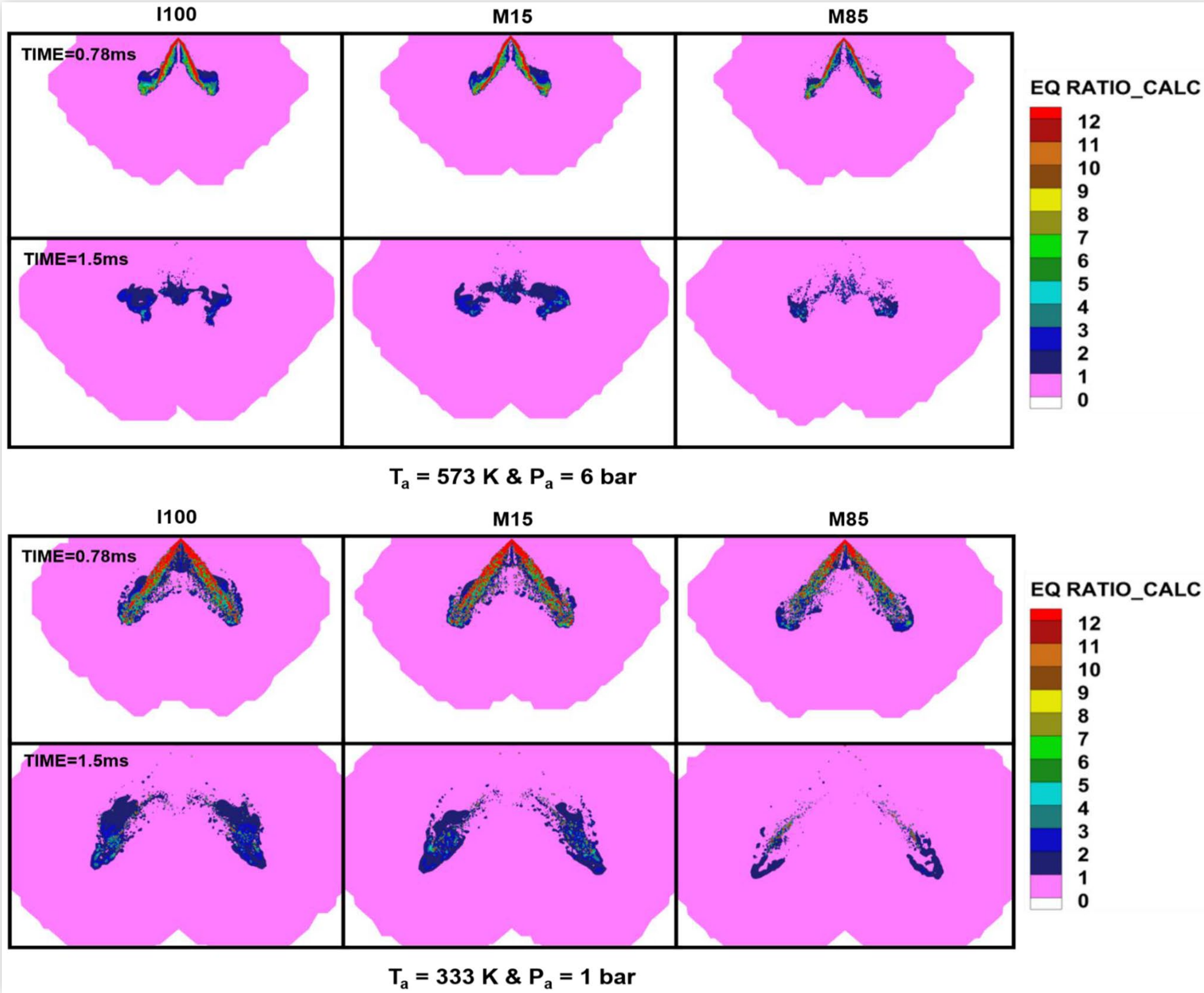

Conclusions

This study was aimed at investigating the spray characteristics and subsequent fuel-air mixing for methanol-iso-octane blends vis-à-vis only-iso-octane (surrogate of gasoline) at two most common engine-like conditions of a GDI engine, resembling early injection and late injection conditions. Simulations were performed using Converge 3.0 CFD software. The premix-ratio of 15% and 85% methanol in iso-octane (v/v) were chosen to examine the effect of fuel properties in different ambient pressure/ temperature conditions. Major inferences drawn from the study are as follows: Spray penetration and SMD of droplets were mainly affected by the ambient pressure/ temperature conditions. These parameters were significantly lower for elevated ambient conditions due to higher drag experienced, improved gas entrainment, and enhanced evaporation of spray droplets. The effect of methanol addition was comparatively lower as compared to ambient conditions. Marginal increase in spray penetration and SMD of droplets was observed for methanol blends due to their higher density, viscosity, and surface tension compared to iso-octane. The effect of fuel properties was suppressed at elevated ambient conditions, which highlighted that methanol blends could be easily adapted in stratified mode of operation without any requirement of injection parameter modifications, although, evaporation characteristics significantly varied for M15 and M85 compared to baseline iso-octane. Methanol blends exhibited inferior and delayed evaporation due to higher vapor pressure and lower volatility of methanol than the iso-octane. However, variation in liquid spray mass for these fuels was more pronounced in high temperature/pressure conditions. Hence, methanol blends required advanced injection timing and higher FIP in the engine compared to iso-octane in order to compensate for delayed mixture formation. Temperature drop due to higher enthalpy of vaporization in methanol blends was more pronounced in lower ambient conditions. Temperature distribution was almost similar for all test fuels in elevated ambient conditions. Cooling effect due to enhanced vaporization of iso-octane under such conditions compensated the temperature drop caused in methanol blends due to higher LHV. Despite lower evaporation rate of methanol blends, equivalence ratio distribution was more aligned towards the stoichiometric due to presence of fuel-bound oxygen in methanol. Hence, utilizing methanol blends would definitely reduce the fuel-rich zone, which would reduce soot formation in GDI engines. This study would surely help improve our understanding of spray behavior of methanol-iso-octane blends under varying ambient conditions. Subsequently, it helps improve engine control parameter optimization for adapting these fuels for IC engine applications.

References

1. Lee, Z., Kim, T., Park, S., and Park, S., "Review on Spray, Combustion, and Emission Characteristics of Recent Developed Direct-Injection Spark Ignition (DISI) Engine System with Multi-Hole Type Injector," *Fuel* 259:116209, 2020.
2. Duronio, F., De Vita, A., Allocca, L., and Anatone, M., "Gasoline Direct Injection Engines-A Review of Latest Technologies and Trends. Part 1: Spray Breakup Process," *Fuel* 265:116948, 2020.
3. Spiegel, L., and Spicher, U., "Mixture Formation and Combustion in a Spark Ignition Engine with Direct Fuel Injection," *SAE Transactions* 967-975, 1992.
4. Storch, M., Pfaffenberger, A., Koegl, M., Will, S., and Zigan, L., "Combustion and Sooting Behavior of Spark-Ignited Ethanol-Iso-Octane Sprays under Stratified Charge Conditions," *Energy & Fuels* 30(7):6080-6090, 2016.
5. Parrish, S.E., and Zink, R.J., "Development and Application of Imaging System to Evaluate Liquid and Vapor Envelopes of Multi-Hole Gasoline Fuel Injector Sprays under Engine-Like Conditions," *Atomization and Sprays* 8:22, 2012.
6. Itani, L.M., Bruneaux, G., Lella, A.D., and Schulz, C., "Two-Tracer LIF Imaging of Preferential Evaporation of Multi-Component Gasoline Fuel Sprays under Engine Conditions," *Proceedings of the Combustion Institute* 35(3):2915-2922, 2015.
7. Moon, S., Li, T., Sato, K., and Yokohata, H., "Governing Parameters and Dynamics of Turbulent Spray Atomization from Modern GDI Injectors," *Energy* 127:89-100, 2017.
8. Lee, S., and Park, S., "Experimental Study on Spray Break-Up and Atomization Processes from GDI Injector Using High Injection Pressure up to 30 MPa," *International Journal of Heat and Fluid Flow* 45:14-22, 2014.
9. Mitroglou, N., Nouri, J.M., Gavaises, M., and Arcoumanis, C., "Spray Characteristics of a Multi-Hole Injector for Direct-Injection Gasoline Engines," *International Journal of Engine Research* 7(3):255-270, 2006.
10. Hoffmann, G., Befrui, B., Berndorfer, A., Piock, W.F., and Varble, D.L., "Fuel System Pressure Increase for Enhanced Performance of GDi Multi-Hole Injection Systems," *SAE International Journal of Engines* 7(1):519-527, 2014.
11. Tian, J., Zhao, M., Long, W., Nishida, K. et al., "Experimental Study on Spray Characteristics under Ultra-High Injection Pressure for DISI Engines," *Fuel* 186:365-374, 2016.
12. Mojtabi, M., Wigley, G., and Helie, J., "The Effect of Flash Boiling on the Atomization Performance of Gasoline Direct Injection Multistream Injectors," *Atomization and Sprays* 6:24, 2014.
13. Yang, S., Song, Z., Wang, T., and Yao, Z., "An Experiment Study on Phenomenon and Mechanism of Flash Boiling Spray from a Multi-Hole Gasoline Direct Injector," *Atomization and Sprays* 5:23, 2013.
14. Guo, H., Ding, H., Li, Y., Ma, X. et al., "Comparison of Spray Collapses at Elevated Ambient Pressure and Flash Boiling Conditions Using Multi-Hole Gasoline Direct Injector," *Fuel* 199:125-134, 2017.
15. Gravalos, Ioannis, Moshou, Dimitrios, Gialamas, Theodoros, Xyradakis, Panagiotis, Kateris, Dimitrios, and Tsiropoulos, Zisis. "Performance and Emission Characteristics of Spark Ignition Engine Fuelled with Ethanol and Methanol Gasoline Blended Fuels." Alternat.
16. Kalwar, A., Singh, A.P., and Agarwal, A.K., "Utilization of Primary Alcohols in Dual-Fuel Injection Mode in a Gasoline Direct Injection Engine," *Fuel* 276, 118068, 2020.
17. Abu-Zaid, M., Badran, O., and Yamin, J., "Effect of Methanol Addition on the Performance of Spark Ignition Engines," *Energy & Fuels* 18(2):312-315, 2004.
18. Sharma, N., and Agarwal, A.K., "Microscopic and Macroscopic Spray Characteristics of GDI Injector Using Gasohol Fuels at Various Injection Pressures," SAE Technical Paper 2016-01-0868, 2016, https://doi.org/10.4271/2016-01-0868.
19. Sonawane, U., Kalwar, A., and Agarwal, A.K., "Microscopic and Macroscopic Spray Characteristics of Gasohols Using a Port Fuel Injection System," SAE Technical Paper 2020-01-0324, 2020, https://doi.org/10.4271/2020-01-0324.
20. Bao, Y., Chan, Q.N., Kook, S., and Hawkes, E., "Spray Penetrations of Ethanol, Gasoline and Iso-Octane in an Optically Accessible Spark-Ignition Direct-Injection Engine," *SAE International Journal of Fuels and Lubricants* 7(3), 2014, https://doi.org/10.4271/2014-01-9079.
21. Kale, R., and Banerjee, R., "Experimental Investigation on GDI Spray Behavior of Iso-Octane and Alcohols at Elevated Pressure and Temperature Conditions," *Fuel* 236:1-12, 2019.
22. Paredi, D., Lucchini, T., D'Errico, G., Onorati, A. et al., "CFD Modeling of Spray Evolution for Spark-Ignition, Direct Injection Engines," *AIP Conference Proceedings* 2191(1):020125, 2019.
23. Paredi, D., Lucchini, T., D'Errico, G., Onorati, A., Pickett, L., and Lacey, J., "Validation of a Comprehensive Computational Fluid Dynamics Methodology to Predict the Direct Injection Process of Gasoline Sprays Using Spray G Experiment."
24. Allocca, L., Bartolucci, L., Cordiner, S., Lazzaro, M. et al., "ECN Spray G Injector: Assessment of Numerical Modeling Accuracy. No. 2018-01-0306," SAE Technical Paper 2018-01-0306, 2018, https://doi.org/10.4271/2018-01-0306.
25. Engine Combustion Network webpage, ecn.sandia.gov.

26. Hwang, J., Weiss, L., Karathanassis, I.K., Koukouvinis, P., Pickett, L.M., and Skeen, S.A., "Spatio-Temporal Identification of Plume Dynamics by 3D Computed Tomography Using Engine Combustion Network Spray G Injector and Various Fuels."
27. Krämer, M., Kull, E., Heldmann, M., and Wensing, M., "Investigations on Gasoline Spray Propagation Behaviour Characteristic for Multihole Injectors," SAE Technical Paper 2014-01-2732, 2014, https://doi.org/10.4271/2014-01-2732.
28. Manin, J., Jung, Y., Skeen, S.A., Pickett, L.M. et al., "Experimental Characterization of DI Gasoline Injection Processes," SAE Technical Paper 2015-01-1894, 2015, https://doi.org/10.4271/2015-01-1894.
29. Payri, R., Salvador, F.J., Martí-Aldaraví, P., and Vaquerizo, D., "ECN Spray G External Spray Visualization and Spray Collapse Description through Penetration and Morphology Analysis," *Applied Thermal Engineering* 112:304-316, 2017.

Contact Information

Prof. Avinash K. Agarwal
Department of Mechanical Engineering
Indian Institute of Technology Kanpur,
Kanpur-208016 India
Tel: +91 512 2597982 (Off)
akag@iitk.ac.in

Acknowledgements

Authors are grateful to Engine Combustion Network (ECN) for making their database available in open domain, which was used in this study.

Definitions/Abbreviations

GDI - Gasoline Direct Injection
CFD - Computational Fluid Dynamics
ECN - Engine Combustion Network
SMD - Sauter Mean Diameter
PM - Particulate Matter
PN - Particulate Number
HC - Hydrocarbons
SOI - Start of Injection
LHV - Latent Heat of Vaporization

ISSN 0148-7191